

Diffractive photon production in γp and $\gamma\gamma$ interactions

N.G.Evanson¹ and J.R.Forshaw^{2*}

¹Department of Physics and Astronomy,
University of Manchester,
Manchester, M13 9PL. England.

²Theory Division, CERN,
1211 Geneva 23. Switzerland.

Abstract

We study the diffractive production of photons in γp and $\gamma\gamma$ collisions. We specifically compute the rates for $\gamma^* p \rightarrow \gamma X$ and for $\gamma^* \gamma^* \rightarrow \gamma\gamma$, where X denotes the proton dissociation. We focus on the rates at large momentum transfers, $-t \gg \Lambda^2$, where we are most confident in the use of QCD perturbation theory. However, our calculations do allow us to study the $-t \rightarrow 0$ behaviour of the $\gamma^* \gamma^* \rightarrow \gamma\gamma$ process in the region where the incoming photons are sufficiently virtual.

PACS numbers: 13.60-r, 13.60.Fz, 13.85-t, 13.85.Dz.

CERN-TH/99-51
February 1999

*On leave of absence from ¹.

1 Introduction

One of the major challenges in the domain of strong interaction dynamics is to gain an understanding of diffractive phenomena within the framework of QCD. Typically, diffractive processes are driven by dynamics at low momentum transfers and hence cannot be studied using perturbation theory.

Large- t diffraction has been shown to be one area where perturbation theory can be used [1]. Double dissociation in hadron-hadron and photon-hadron collisions with a large momentum transfer between the diffracting systems has been, and continues to be, studied both theoretically [2, 3] and experimentally [4]. The large momentum transfer means that jets are produced in the diffracting systems, the identification of which leads to a sample of ‘gaps between jets’ events. A reliable calculation of the expected rate for double dissociation is made difficult because there is the possibility of additional strong interactions between the diffracting systems which could result in the loss of gaps. A process which avoids the ‘gap survival’ problem is diffractive vector meson production in photon-hadron collisions: $\gamma p \rightarrow VX$ [5, 6, 7, 8]. The meson V is produced with a high p_t relative to the incoming photon and the largeness of this momentum transfer typically leads to the dissociation of the hadron into system X . A principal challenge in computing the rate for meson production lies in determining how the meson is produced. To avoid both the meson wavefunction problem and the gap survival problem, one can study the diffractive production of photons [5, 6, 9]. At HERA, one can look for $\gamma p \rightarrow \gamma X$ where the photon is produced with a high p_t and the proton dissociates. At LEP2 or a future linear collider one can look for $\gamma\gamma \rightarrow \gamma X$ or $\gamma\gamma \rightarrow \gamma\gamma$ [5, 10]. In this paper we compute the rates for diffractive photon production in photon-proton and photon-photon collisions at large momentum transfer. Our calculations include the possibility of off-shell incoming photons.

2 The $\gamma^*\gamma$ impact factor

The scattering amplitude in the high energy (Regge) limit may be factorised in the following way

$$A(s, t) = \frac{is}{(2\pi)^4} G \int d^2\mathbf{k}_1 d^2\mathbf{k}_2 \Phi_1(\mathbf{k}_1, \mathbf{q}) \Phi_2(\mathbf{k}_2, \mathbf{q}) f(s, \mathbf{k}_1, \mathbf{k}_2, \mathbf{q}). \quad (2.1)$$

G is the colour factor for the process and the functions $\Phi_i(\mathbf{k}_i, \mathbf{q})$ are the impact factors which contain the information about the external hadronic states. The function $f(s, \mathbf{k}_1, \mathbf{k}_2, \mathbf{q})$ contains all the internal dynamics of the BFKL pomeron, is process independent and is well known in the leading logarithm approximation (LLA) which we use throughout [11, 12]. The corresponding differential cross-section is

$$\frac{d\sigma}{dt} = \frac{|A(s, t)|^2}{16\pi s^2}. \quad (2.2)$$

For diffractive photon production we need to compute the $\gamma^*\gamma$ impact factor. The relevant Feynman diagrams are shown in Fig. 1. Dispersive techniques are used to calculate the imaginary part of the amplitude which is all that is required in the LLA. The study of the the photon impact factor is not new and dates back to [13]. In this paper, we compute the impact factor with an off-shell incoming photon and a general momentum transfer.

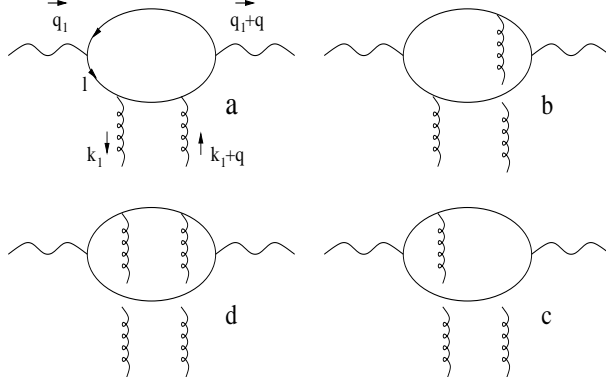


Figure 1: The four diagrams that contribute to the photon-photon impact factor

We detail the calculation of the contribution to the impact factor arising from the amplitude of Fig.1(a). The same techniques apply to all diagrams.

$$(A_{(a)}^{jk})^{\mu\nu} = -(4\pi)^2 \alpha_s \alpha \sum_q e_q^2 \int d(PS) \frac{\text{Tr}(\not{l} \gamma^\mu (\not{l} - \not{k}_1) \gamma^\nu (\not{l} + \not{q}) \not{\epsilon}_{(f)}^k (\not{l} - \not{q}_1) \not{\epsilon}_{(i)}^j)}{l^2 (l+q)^2}. \quad (2.3)$$

The photon polarisation states are labelled by j and k and $d(PS)$ refers to the two-body phase space of the cut quark lines shown in Fig.1. We define two light-like and mutually orthogonal vectors, p_1 and p_2 . All momenta are then Sudakov decomposed into components proportional to p_1 , and p_2 and a third perpendicular vector:

$$\begin{aligned} q_1^\mu &= p_1^\mu - \frac{Q^2}{s} p_2^\mu \\ l^\mu &= \rho p_1^\mu + \lambda p_2^\mu + l_\perp^\mu \\ k_1^\mu &= \rho_1 p_1^\mu + \lambda_1 p_2^\mu + k_{1\perp}^\mu \\ q^\mu &= \rho_t p_1^\mu + \lambda_t p_2^\mu + q_\perp^\mu. \end{aligned} \quad (2.4)$$

q_1 is the incoming photon momentum ($Q^2 = -q_1^2$), l the quark momentum, $k_1 + q$ and $-k_1$ are the momenta of the gluon legs. The momentum transfer is $q^2 = t < 0$. Working in the eikonal approximation we are only interested in terms that are proportional to $p_1^\mu p_1^\nu$ in the numerator of (2.3). Projecting out this piece, the amplitude becomes

$$(A_{(a)}^{jk})^{\mu\nu} = -(4\pi)^2 \frac{4}{s^2} \alpha_s \alpha \sum_q e_q^2 \int d(PS) \frac{\text{Tr}(\not{l} \not{p}_2 (\not{l} - \not{k}_1) \not{p}_2 (\not{l} + \not{q}) \not{\epsilon}_{(f)}^k (\not{l} - \not{q}_1) \not{\epsilon}_{(i)}^j)}{l^2 (l+q)^2} p_1^\mu p_1^\nu. \quad (2.5)$$

The two-body phase space integration over the cut lines is

$$\begin{aligned} \int d(PS) &= \int \frac{d^4 l}{(2\pi)^3} \frac{d^4 k_1}{(2\pi)^3} \delta((l - k_1)^2) \delta((q_1 - l)^2) \\ &= \left(\frac{s}{2}\right)^2 \int d\rho \, d\lambda \, d\rho_1 \, d\lambda_1 \int \frac{d^2 \mathbf{l}}{(2\pi)^3} \frac{d^2 \mathbf{k}_1}{(2\pi)^3} \frac{-1}{\rho(1-\rho)s^2} \delta\left(\lambda - \lambda_1 - \frac{(1 - \mathbf{k}_1)^2}{s\rho}\right) \\ &\times \delta\left(\lambda + \frac{Q^2}{s} + \frac{\mathbf{l}^2}{s(1-\rho)}\right). \end{aligned} \quad (2.6)$$

We have used the fact that $\rho_1 \ll \rho$ in the LLA and have transferred from the Minkowski metric to the Euclidean one:

$$-(k_{1\perp}^\mu)^2 = \mathbf{k}_1^2. \quad (2.7)$$

The δ functions are used to absorb the λ and λ_1 integrals and lead to

$$\begin{aligned} q_1^\mu &= p_1^\mu - Q^2 \frac{p_2^\mu}{s} \\ l^\mu &= \rho p_1^\mu - \left(\frac{\mathbf{l}^2}{(1-\rho)} + Q^2 \right) \frac{p_2^\mu}{s} + l_\perp^\mu \\ k_1^\mu &= - \left(\frac{(\mathbf{k}_1 - \mathbf{l})^2}{\rho} + Q^2 + \frac{\mathbf{l}^2}{(1-\rho)} \right) \frac{p_2^\mu}{s} + k_{1\perp}^\mu \\ q^\mu &= (Q^2 + \mathbf{q}^2) \frac{p_2^\mu}{s} + q_\perp^\mu. \end{aligned} \quad (2.8)$$

Within the LLA it is safe to neglect ρ_1 and ρ_t .

Our notation follows that of [14], and so we can readily extract the corresponding impact factor by removing the

$$\frac{2p_1^\mu p_1^\nu}{(2\pi)^4} \int d\rho_1 d^2 \mathbf{k}_1$$

from (2.5), i.e.

$$\Phi_{(a)}^{jk}(\mathbf{k}_1, \mathbf{q}) = -\frac{2\alpha\alpha_s}{s^2} \sum_q e_q^2 \int d^2 \mathbf{l} \int_0^1 d\rho \frac{T_{(a)}^{jk}}{\rho(1-\rho)} \quad (2.9)$$

where $T_{(a)}^{jk}$ is given by

$$T_{(a)}^{jk} = \frac{\text{Tr}(\not{l} \not{p}_2 (\not{l} - \not{k}_1) \not{p}_2 (\not{l} + \not{q}) \not{\epsilon}_{(f)}^k (\not{l} - \not{q}_1) \not{\epsilon}_{(i)}^j)}{l^2(l+q)^2}. \quad (2.10)$$

It is not necessary to calculate the contributions to the impact factor from all four diagrams explicitly since they are related to each other by the transformations shown in Fig.2.

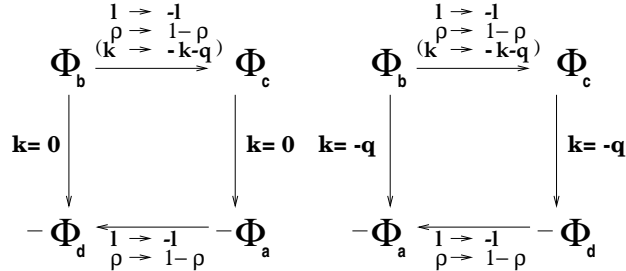


Figure 2: The relationship between the four amplitudes of Fig.1

Thus, the full impact factor is given by

$$\Phi_{\gamma\gamma}^{jk}(\mathbf{k}_1, \mathbf{q}) = -\alpha\alpha_s \left(\frac{2}{s} \right)^2 \sum_q e_q^2 \int d^2 \mathbf{l} \int_0^1 d\rho \frac{1}{\rho(1-\rho)} \left[T_{(c)}^{jk} - T_{(c)}^{jk}|_{\mathbf{k}_1=0} \right] \quad (2.11)$$

where

$$T_{(c)}^{jk} = \frac{\text{Tr}(\not{l} \not{p}_2 (\not{l} + \not{k}_1 + \not{q}) \not{\epsilon}_{(f)}^k (\not{l} - \not{q}_1 + \not{k}_1) \not{p}_2 (\not{l} - \not{q}_1) \not{\epsilon}_{(i)}^j)}{(l - q_1)^2 (l + k_1 + q)^2}. \quad (2.12)$$

2.1 Photon polarisation

The transverse polarisation vectors of the incoming photon lie in the transverse plane by definition. However, as the final state photon gets a kick into the transverse plane, its polarisation vectors have a component in the non-transverse directions. In the Lorentz gauge, the most general polarisation vectors for the incoming and outgoing photons are

$$\begin{aligned} \epsilon_{(f)}^{k\mu} &= \epsilon_{\perp}^{k\mu} - \frac{2 q_{\perp} \cdot \epsilon_{\perp}^k}{s} p_2^{\mu}, \\ \epsilon_{(i)}^{j\mu} &= \epsilon_{\perp}^{j\mu}. \end{aligned} \quad (2.13)$$

Placing these polarisation vectors into the amplitude and taking the trace [15] we get

$$\begin{aligned} \Phi_{(x)}^{jk}(\mathbf{k}_1, \mathbf{q}) &= \pm 4\alpha_s \alpha \sum_q e_q^2 \int_0^1 d\rho \int d^2\mathbf{l} \frac{1}{(\mathbf{l}^2 + \overline{Q}^2)} \\ &\frac{\Delta_{(x)} \cdot \epsilon^{*k} \mathbf{l} \cdot \epsilon^j (1 - 2\rho)^2 - \epsilon^{*k} \cdot \epsilon^j \mathbf{l} \cdot (\mathbf{l} - \Delta_{(x)}) + 4\mathbf{l} \cdot \epsilon^{*k} \mathbf{l} \cdot \epsilon^j \rho(1 - \rho) - \mathbf{l} \cdot \epsilon^{*k} \Delta_{(x)} \cdot \epsilon^j}{(\Delta_{(x)} - \mathbf{l})^2}. \end{aligned} \quad (2.14)$$

$x = a, b, c, d$ labels the diagram in Fig.1. The impact factor takes the + sign for diagrams (b) and (c) and the - sign for diagrams (a) and (d). We are focusing on diagram (c), in which case

$$\Delta_{(c)} = \mathbf{k}_1 + \rho \mathbf{q}.$$

All boldface vectors are Euclidean and lie in the transverse plane, e.g. $\epsilon^{j2} = -\epsilon_{\perp}^{j2}$. We have also introduced $\overline{Q}^2 \equiv Q^2 \rho(1 - \rho)$.

The longitudinal polarisation vector of the incoming photon is given by

$$\epsilon^{0\mu} = \frac{1}{\sqrt{Q^2}} p_1^{\mu} + \frac{\sqrt{Q^2}}{s} p_2^{\mu}. \quad (2.15)$$

After substituting this expression into the amplitude and taking the trace:

$$\Phi_{(x)}^{0i}(\mathbf{k}_1, \mathbf{q}) = \frac{\pm 4\alpha_s \alpha}{Q} \sum_q e_q^2 \int_0^1 d\rho (2\rho - 1) \int d^2\mathbf{l} \frac{(\mathbf{l}^2 - \overline{Q}^2)}{(\mathbf{l}^2 + \overline{Q}^2)} \frac{(\Delta_{(x)} - \mathbf{l}) \cdot \epsilon_i}{(\Delta_{(x)} - \mathbf{l})^2} \quad (2.16)$$

which is identically zero. Thus, in the LLA, longitudinally polarised photons do not scatter into real photons.

2.2 Impact factor in position space

The four-gluon amplitude, $f(s, \mathbf{k}_1, \mathbf{k}_2, \mathbf{q})$ of (2.1), can be written [12]:

$$f(s, \mathbf{k}_1, \mathbf{k}_2, \mathbf{q}) = \frac{1}{(2\pi)^6} \int d^2 \rho_1 d^2 \rho_2 d^2 \rho_3 d^2 \rho_4 e^{-i(\mathbf{k}_1 \cdot \rho_1 - (\mathbf{k}_1 + \mathbf{q}) \cdot \rho_2 - \mathbf{k}_2 \cdot \rho_3 + (\mathbf{k}_2 + \mathbf{q}) \cdot \rho_4)} \int_{-\infty}^{\infty} d\nu \frac{\nu^2}{(\nu^2 + 1/4)^2} e^{z\chi(\nu)} E^\nu(\rho_1, \rho_2) E^{*\nu}(\rho_3, \rho_4). \quad (2.17)$$

We have neglected the contributions with conformal spin $n > 0$ since they give rise to sub-leading contributions at high energies. The eigenfunctions of the kernel are given explicitly by

$$E^\nu(\rho_1, \rho_2) = \left| \frac{\rho_1 - \rho_2}{\rho_1 \rho_2} \right|^{1+2i\nu}, \quad (2.18)$$

$$\chi(\nu) = 2\Psi(1) - \Psi(1/2 + i\nu) - \Psi(1/2 - i\nu) \quad (2.19)$$

($\Psi(x)$ is the digamma function) and

$$z = \frac{N_c \alpha_s}{\pi} \ln \left(\frac{s}{s_0} \right). \quad (2.20)$$

The choice of scale s_0 is arbitrary in the LLA, in our subsequent calculations we choose either the largest scale (apart from s) in the problem or set a value for z . The number of colours, $N_c = 3$.

The scattering amplitude (2.1) can now be written

$$A(s, t) = \frac{is G}{(2\pi)^{10}} \int_{-\infty}^{\infty} d\nu \frac{\nu^2}{(\nu^2 + 1/4)^2} e^{z\chi(\nu)} I_1^\nu I_2^{*\nu} \quad (2.21)$$

and we have introduced the functions

$$I_i^\nu = \int d^2 \mathbf{k}_1 \Phi_i(\mathbf{k}_1, \mathbf{q}) \int d^2 \rho_1 d^2 \rho_2 E^\nu(\rho_1, \rho_2) e^{-i\mathbf{k}_1 \cdot (\rho_1 - \rho_2) + i\mathbf{q} \cdot \rho_2}. \quad (2.22)$$

For photon production we need to calculate (2.22) using $\Phi_{\gamma\gamma}^{jk}$. We work in the helicity basis:

$$\epsilon^\pm = -\frac{1}{\sqrt{2}}(1, \pm i). \quad (2.23)$$

There are four amplitudes to consider: $(j, k) = (+, +), (+, -), (-, +), (-, -)$ and

$$\Phi_{(x)}^{(-, -)}(\mathbf{k}_1, \mathbf{q}) = 4\alpha\alpha_s \sum_q e_q^2 \int_0^1 d\rho (\rho^2 + (1 - \rho)^2) \int d^2 \mathbf{l} \frac{1}{(\mathbf{l}^2 + \overline{Q}^2)} \frac{\Delta_{(x)}^* l - \mathbf{l}^2}{(\Delta_{(x)} - 1)^2} \quad (2.24)$$

From now on, non-boldface momenta are understood to be complex numbers, e.g. $l = l_x + il_y$. To compute $I_{(-, -)}^\nu$ we first take the Fourier transform of the impact factor:

$$\Phi_{(x)}^{(-, -)}(\rho_1, \rho_2) = e^{i\mathbf{q} \cdot \rho_2} \int d^2 \mathbf{k}_1 \Phi_{(x)}^{(-, -)}(\mathbf{k}_1, \mathbf{q}) e^{-i\mathbf{k}_1 \cdot (\rho_1 - \rho_2)}. \quad (2.25)$$

Summing over all four diagrams gives

$$\begin{aligned} \Phi_{(-, -)}(\rho_1, \rho_2) &= 4\alpha\alpha_s \sum_q e_q^2 \int_0^1 d\rho (\rho^2 + (1 - \rho)^2) \int d^2 \mathbf{k}_1 d^2 \mathbf{k}_2 e^{-i\mathbf{k}_1 \cdot \rho_1} e^{i\mathbf{k}_2 \cdot \rho_2} \\ &\quad \delta^2(\mathbf{k}_2 - \mathbf{k}_1 - \mathbf{q}) \int d^2 \mathbf{l} d^2 \mathbf{l}' \frac{l'^* l}{(\mathbf{l}^2 + \overline{Q}^2) \mathbf{l}'^2} \left[\delta^2(\mathbf{l}' + \mathbf{l} - \mathbf{k}_1 - \rho \mathbf{q}) \right. \\ &\quad \left. - \delta^2(\mathbf{l}' - \mathbf{l} - \mathbf{k}_1 - (1 - \rho) \mathbf{q}) - \delta^2(\mathbf{l}' + \mathbf{l} - \rho \mathbf{q}) + \delta^2(\mathbf{l}' - \mathbf{l} - (1 - \rho) \mathbf{q}) \right]. \end{aligned} \quad (2.26)$$

Equivalently, and dropping for the time being the pre-factors and the integral over the momentum fraction ρ , we have

$$\int \frac{d^2 \mathbf{r}_1 d^2 \mathbf{r}_2}{(2\pi)^4} \int d^2 \mathbf{k}_1 d^2 \mathbf{k}_2 e^{-i\mathbf{k}_1 \cdot \boldsymbol{\rho}_1} e^{i\mathbf{k}_2 \cdot \boldsymbol{\rho}_2} e^{i\mathbf{r}_1 \cdot (\mathbf{k}_2 - \mathbf{k}_1 - \mathbf{q})} \int d^2 \mathbf{l} d^2 \mathbf{l}' \frac{l'^* l}{(\mathbf{l}^2 + \overline{Q}^2) \mathbf{l}'^2} \left[e^{-i\mathbf{r}_2 \cdot (\mathbf{l}' + \mathbf{l} - \mathbf{k}_1 - \rho \mathbf{q})} - e^{i\mathbf{r}_2 \cdot (\mathbf{l}' - \mathbf{l} - \mathbf{k}_1 - (1-\rho)\mathbf{q})} - e^{i\mathbf{r}_2 \cdot (\mathbf{l}' + \mathbf{l} - \rho \mathbf{q})} + e^{i\mathbf{r}_2 \cdot (\mathbf{l}' - \mathbf{l} - (1-\rho)\mathbf{q})} \right]. \quad (2.27)$$

After some algebra, this becomes

$$\epsilon_a^- \epsilon_b^+ \int \frac{d^2 \mathbf{r}_1 d^2 \mathbf{r}_2}{(2\pi)^4} e^{-i\mathbf{r}_1 \cdot \mathbf{q}} \int d^2 \mathbf{k}_1 d^2 \mathbf{k}_2 \left[e^{i\mathbf{k}_1 \cdot (\mathbf{r}_1 + \mathbf{r}_2 + \boldsymbol{\rho}_1)} - e^{-i\mathbf{k}_1 \cdot (\mathbf{r}_1 + \boldsymbol{\rho}_1)} \right] e^{i\mathbf{k}_2 \cdot (\mathbf{r}_1 + \boldsymbol{\rho}_2)} \left[e^{-i\mathbf{r}_2 \cdot \rho \mathbf{q}} \left(\frac{\nabla_{\mathbf{r}_2}^a}{i} \int d^2 \mathbf{l} \frac{e^{i\mathbf{r}_2 \cdot \mathbf{l}}}{\mathbf{l}^2 + \overline{Q}^2} \right) - e^{-i\mathbf{r}_2 \cdot (1-\rho)\mathbf{q}} \left(\frac{\nabla_{\mathbf{r}_2}^a}{-i} \int d^2 \mathbf{l} \frac{e^{-i\mathbf{r}_2 \cdot \mathbf{l}}}{\mathbf{l}^2 + \overline{Q}^2} \right) \right] \frac{\nabla_{\mathbf{r}_2}^b}{i} \int d^2 \mathbf{l}' \frac{e^{-i\mathbf{r}_2 \cdot \mathbf{l}'}}{\mathbf{l}'^2} \quad (2.28)$$

where a and b are vector indices in the transverse space. Performing the angular parts of the \mathbf{l} and \mathbf{l}' integrals and the \mathbf{k}_1 and \mathbf{k}_2 integrals yields

$$-\epsilon_a^- \epsilon_b^+ (2\pi)^2 \int d^2 \mathbf{r}_1 d^2 \mathbf{r}_2 \left[e^{-i\mathbf{r}_2 \cdot \rho \mathbf{q}} + e^{-i\mathbf{r}_2 \cdot (1-\rho)\mathbf{q}} \right] e^{-i\mathbf{r}_1 \cdot \mathbf{q}} \left(\nabla_{\mathbf{r}_2}^a \int d|\mathbf{l}| \frac{|\mathbf{l}| J_0(|\mathbf{r}_2||\mathbf{l}|)}{\mathbf{l}^2 + \overline{Q}^2} \right) \left(\nabla_{\mathbf{r}_2}^b \int d|\mathbf{l}'| \frac{J_0(|\mathbf{r}_2||\mathbf{l}'|)}{|\mathbf{l}'|} \right) \left[\delta^2(\mathbf{r}_1 + \mathbf{r}_2 + \boldsymbol{\rho}_1) - \delta^2(\mathbf{r}_1 + \boldsymbol{\rho}_1) \right] \delta^2(\mathbf{r}_1 + \boldsymbol{\rho}_2). \quad (2.29)$$

Using

$$\nabla_{\mathbf{r}_2} J_0(|\mathbf{r}_2||\mathbf{l}|) = -|\mathbf{l}| J_1(|\mathbf{r}_2||\mathbf{l}|) \hat{\mathbf{r}}_2, \quad (2.30)$$

$$\boldsymbol{\epsilon}^+ \cdot \hat{\mathbf{r}}_2 \boldsymbol{\epsilon}^- \cdot \hat{\mathbf{r}}_2 = 1, \quad (2.31)$$

completing the radial \mathbf{l} integral and re-arranging leads to the result:

$$\Phi_{(-,-)}(\boldsymbol{\rho}_1, \boldsymbol{\rho}_2) = 16\pi^2 \alpha \alpha_s \sum_q e_q^2 \int_0^1 d\rho [\rho^2 + (1-\rho)^2] \int d^2 \mathbf{r}_1 d^2 \mathbf{r}_2 \frac{1}{|\mathbf{r}|} e^{i\rho \mathbf{q} \cdot \mathbf{r}_1} e^{i(1-\rho)\mathbf{q} \cdot \mathbf{r}_2} \overline{Q} K_1(|\mathbf{r}|\overline{Q}) [\delta^2(\mathbf{r}_1 - \boldsymbol{\rho}_1) - \delta^2(\mathbf{r}_2 - \boldsymbol{\rho}_1)] [\delta^2(\mathbf{r}_1 - \boldsymbol{\rho}_2) - \delta^2(\mathbf{r}_2 - \boldsymbol{\rho}_2)], \quad (2.32)$$

where $\mathbf{r} = \mathbf{r}_1 - \mathbf{r}_2$. The impact factors for the other polarisation states are

$$\begin{aligned} \Phi_{(+,+)}(\boldsymbol{\rho}_1, \boldsymbol{\rho}_2) &= \Phi_{(-,-)}(\boldsymbol{\rho}_1, \boldsymbol{\rho}_2) \\ \Phi_{(+,-)}(\boldsymbol{\rho}_1, \boldsymbol{\rho}_2) &= 32\pi^2 \alpha \alpha_s \sum_q e_q^2 \int_0^1 d\rho \int d^2 \mathbf{r}_1 d^2 \mathbf{r}_2 \rho(1-\rho) \frac{r^2}{|\mathbf{r}|^3} e^{i\rho \mathbf{q} \cdot \mathbf{r}_1} e^{i(1-\rho)\mathbf{q} \cdot \mathbf{r}_2} \\ &\quad K_1(|\mathbf{r}|\overline{Q}) \overline{Q} [\delta^2(\mathbf{r}_1 - \boldsymbol{\rho}_1) - \delta^2(\mathbf{r}_2 - \boldsymbol{\rho}_1)] [\delta^2(\mathbf{r}_1 - \boldsymbol{\rho}_2) - \delta^2(\mathbf{r}_2 - \boldsymbol{\rho}_2)] \\ \Phi_{(-,+)}(\boldsymbol{\rho}_1, \boldsymbol{\rho}_2) &= 32\pi^2 \alpha \alpha_s \sum_q e_q^2 \int_0^1 d\rho \int d^2 \mathbf{r}_1 d^2 \mathbf{r}_2 \rho(1-\rho) \frac{r^{*2}}{|\mathbf{r}|^3} e^{i\rho \mathbf{q} \cdot \mathbf{r}_1} e^{i(1-\rho)\mathbf{q} \cdot \mathbf{r}_2} \\ &\quad K_1(|\mathbf{r}|\overline{Q}) \overline{Q} [\delta^2(\mathbf{r}_1 - \boldsymbol{\rho}_1) - \delta^2(\mathbf{r}_2 - \boldsymbol{\rho}_1)] [\delta^2(\mathbf{r}_1 - \boldsymbol{\rho}_2) - \delta^2(\mathbf{r}_2 - \boldsymbol{\rho}_2)]. \end{aligned} \quad (2.33)$$

3 Projection on Conformal Eigenstates

We must now project the position space impact factors onto the conformal eigenfunctions of the BFKL kernel, i.e. we must perform the following convolution:

$$I_{(h_\gamma^*, h_\gamma)}^\nu(Q^2, q^2) = \int d^2 \rho_1 d^2 \rho_2 \Phi_{(h_\gamma^*, h_\gamma)}(\rho_1, \rho_2) E^\nu(\rho_1, \rho_2). \quad (3.34)$$

This part of the calculation follows very closely that of [9]. For completeness, we reproduce the steps here.

In two of the terms of (2.33) the δ -functions force $\rho_1 = \rho_2$ which results in a vanishing contribution due to the vanishing of E^ν . Hence,

$$\begin{aligned} I_{(+,+)}^\nu(Q^2, q^2) &= -32\pi^2 \alpha_s \alpha \sum_q e_q^2 \int_0^1 d\rho [\rho^2 + (1-\rho)^2] \overline{Q} \\ &\int d^2 \mathbf{r}_1 d^2 \mathbf{r}_2 \frac{1}{|\mathbf{r}|} K_1(|\mathbf{r}| \overline{Q}) e^{i\rho \mathbf{q} \cdot \mathbf{r}_1} e^{i(1-\rho) \mathbf{q} \cdot \mathbf{r}_2} \left| \frac{\mathbf{r}}{\mathbf{r}_1 \mathbf{r}_2} \right|^{1+2i\nu} \end{aligned} \quad (3.35)$$

i.e.

$$\begin{aligned} I_{(+,+)}^\nu(Q^2, q^2) &= -32\pi^2 \alpha_s \alpha \sum_q e_q^2 \int_0^1 d\rho [\rho^2 + (1-\rho)^2] \overline{Q} \\ &\int d^2 \mathbf{r} d^2 \mathbf{r}_2 e^{i\rho \mathbf{q} \cdot \mathbf{r}} e^{i\mathbf{q} \cdot \mathbf{r}_2} |\mathbf{r}|^{2i\nu} K_1(|\mathbf{r}| \overline{Q}) |(\mathbf{r} + \mathbf{r}_2) \cdot \mathbf{r}_2|^{-1-2i\nu}. \end{aligned} \quad (3.36)$$

We next shift \mathbf{r}_2 by $-\rho \mathbf{r}$ to eliminate the \mathbf{r} dependent phase factor:

$$\begin{aligned} I_{(+,+)}^\nu(Q^2, q^2) &= -32\pi^2 \alpha_s \alpha \sum_q e_q^2 \int_0^1 d\rho [\rho^2 + (1-\rho)^2] \overline{Q} \int d^2 \mathbf{r} d^2 \mathbf{r}_2 e^{i\mathbf{q} \cdot \mathbf{r}_2} \\ &K_1(|\mathbf{r}| \overline{Q}) |\mathbf{r}|^{2i\nu} |[\mathbf{r}_2 + (1-\rho)\mathbf{r}] [\mathbf{r}_2 - \rho \mathbf{r}]|^{-1-2i\nu}. \end{aligned} \quad (3.37)$$

We now switch to the complex notation, i.e from $\mathbf{r} = (r_1, r_2)$ to $a = r_1 + i r_2$ and $b = r_1 - i r_2$, and use the freedom to choose q to be real:

$$\begin{aligned} I_{(+,+)}^\nu(Q^2, q^2) &= -8\pi^2 \alpha_s \alpha \sum_q e_q^2 \int_0^1 d\rho [\rho^2 + (1-\rho)^2] \overline{Q} \int da db da_2 db_2 e^{iq/2(a_2+b_2)} \\ &(ab)^{i\nu} K_1(\sqrt{ab \overline{Q}^2}) \{[a_2 + (1-\rho)a] [b_2 + (1-\rho)b] [a_2 - \rho a][b_2 - \rho b]\}^{-1/2-i\nu}. \end{aligned} \quad (3.38)$$

To proceed we factorise the integration in a, b and a_2, b_2 by writing the Bessel function as its Mellin transform,

$$K_1(x) = \frac{1}{8\pi} \int_{-\infty}^{\infty} d\lambda \left(\frac{x}{2}\right)^{-\gamma-i\lambda} \Gamma\left(\frac{i\lambda + \gamma - 1}{2}\right) \Gamma\left(\frac{i\lambda + \gamma + 1}{2}\right) \quad [\Re \gamma > 1], \quad (3.39)$$

and re-scaling a & b by a_2 & b_2 respectively:

$$\begin{aligned} I_{(+,+)}^\nu(Q^2, q^2) &= -2\pi \alpha_s \alpha \sum_q e_q^2 \int_0^1 d\rho [\rho^2 + (1-\rho)^2] \int_{-\infty}^{\infty} d\lambda (\overline{Q}^2)^{\frac{-\gamma-i\lambda+1}{2}} \\ &2^{\gamma+i\lambda-1} \Gamma\left(\frac{i\lambda + \gamma - 1}{2}\right) \Gamma\left(\frac{i\lambda + \gamma + 1}{2}\right) \int da_2 db_2 e^{iq/2(a_2+b_2)} (a_2 b_2)^{\frac{-\gamma-i\lambda}{2}-i\nu} \\ &\int da db (ab)^{\frac{-\gamma-i\lambda}{2}+i\nu} \{[1 + (1-\rho)a] [1 + (1-\rho)b] [1 - \rho a][1 - \rho b]\}^{-1/2-i\nu}. \end{aligned} \quad (3.40)$$

Re-scaling a_2 and b_2 by $2i/q$ gives

$$\begin{aligned}
I_{(+,+)}^\nu(Q^2, q^2) &= 2\pi\alpha_s\alpha \sum_q e_q^2 \left(\frac{2}{q}\right)^{1-2i\nu} \int_0^1 d\rho [\rho^2 + (1-\rho)^2] \int_{-\infty}^{\infty} d\lambda \left(\frac{\bar{Q}^2}{q^2}\right)^{\frac{-\gamma-i\lambda+1}{2}} \\
&\quad \Gamma\left(\frac{i\lambda+\gamma-1}{2}\right) \Gamma\left(\frac{i\lambda+\gamma+1}{2}\right) \int da_2 db_2 e^{-(a_2+b_2)} (-a_2 b_2)^{\frac{-\gamma-i\lambda}{2}-i\nu} \\
&\quad \int da db (ab)^{\frac{-\gamma-i\lambda}{2}+i\nu} \{[1+(1-\rho)a][1+(1-\rho)b][1-\rho a][1-\rho b]\}^{-1/2-i\nu}. \quad (3.41)
\end{aligned}$$

Completing the a, b and a_2, b_2 integrals as in [9]:

$$\begin{aligned}
&\int da_2 db_2 e^{-(a_2+b_2)} (-a_2 b_2)^{\frac{-\gamma-i\lambda}{2}-i\nu} \\
&= 2i \sin\left[\left(\frac{\gamma+i\lambda}{2} + i\nu\right)\pi\right] \int_0^\infty da_2 a_2^{\frac{-\gamma-i\lambda}{2}-i\nu} e^{-a_2} \int_0^\infty db_2 b_2^{\frac{-\gamma-i\lambda}{2}-i\nu} e^{-b_2} \quad (3.42) \\
&= 2i \sin\left[\left(\frac{\gamma+i\lambda}{2} + i\nu\right)\pi\right] \Gamma^2\left(\frac{-\gamma-i\lambda}{2} - i\nu + 1\right) \\
&\quad \int da db (ab)^{\frac{-\gamma-i\lambda}{2}+i\nu} \{[1+(1-\rho)a][1+(1-\rho)b][1-\rho a][1-\rho b]\}^{-1/2-i\nu} \\
&= 2i \sin\left[(-1/2 - i\nu)\pi\right] \left\{ \int_{-1/(1-\rho)}^0 db \int_{-\infty}^{-1/(1-\rho)} da + \int_0^{1/\rho} db \int_{1/\rho}^\infty da \right\} \\
&\quad (ab)^{\frac{-\gamma-i\lambda}{2}+i\nu} \{ -[1+(1-\rho)a][1+(1-\rho)b][1-\rho a][1-\rho b] \}^{-1/2-i\nu} \\
&= 2i \sin(z_2\pi) [\rho(1-\rho)]^{z_2} (1-\rho)^{-2(1+z_1+z_2)} \int_0^1 db b^{z_1} \left\{ (1-b) \left(1 + \frac{\rho}{1-\rho} b\right) \right\}^{z_2} \\
&\quad \int_1^\infty da a^{z_1} \left\{ (a-1) \left(a + \frac{1-\rho}{\rho}\right) \right\}^{z_2} + [\rho \rightarrow (1-\rho)] \quad (3.43)
\end{aligned}$$

and we have defined

$$\begin{aligned}
z_1 &= \frac{-\gamma-i\lambda}{2} + i\nu \\
z_2 &= -1/2 - i\nu. \quad (3.44)
\end{aligned}$$

The above integrals are representations of the hypergeometric function, i.e. (3.43) can be written

$$\begin{aligned}
&= 4i \sin(z_2\pi) [\rho(1-\rho)]^{z_2} \frac{\Gamma(z_1+1)\Gamma(z_2+1)}{\Gamma(z_1+z_2+2)} \frac{\Gamma(-z_1-2z_2-1)\Gamma(z_2+1)}{\Gamma(-z_1-z_2)} (1-\rho)^{-2(1+z_1+z_2)} \\
&\quad {}_2F_1\left(-z_2, z_1+1; z_1+z_2+2; \frac{\rho}{\rho-1}\right) {}_2F_1\left(-z_2, -z_1-2z_2-1; -z_1-z_2; \frac{\rho-1}{\rho}\right) \quad (3.45)
\end{aligned}$$

and we have anticipated the symmetry between ρ and $(1-\rho)$ when performing the ρ integral. We can further simplify the hypergeometric functions to reach

$$\begin{aligned}
&= -4i \sin((1/2 + i\nu)\pi) \frac{\Gamma^2(1/2 - i\nu) \Gamma(\frac{-\gamma-i\lambda}{2} + i\nu + 1) \Gamma(\frac{\gamma+i\lambda}{2} + i\nu)}{\Gamma(\frac{\gamma+i\lambda+1}{2}) \Gamma(\frac{-\gamma-i\lambda+3}{2})} (1-\rho)^{-1+\gamma+i\lambda} \\
&\quad {}_2F_1\left(1/2 + i\nu, 1/2 - i\nu; \frac{-\gamma-i\lambda+3}{2}; \rho\right) {}_2F_1\left(1/2 + i\nu, 1/2 - i\nu; \frac{\gamma+i\lambda+1}{2}; 1-\rho\right). \quad (3.46)
\end{aligned}$$

Using these integrals, (3.41) reduces to

$$\begin{aligned}
I_{(+,+)}^\nu(Q^2, q^2) &= 16\pi^3 \alpha_s \alpha \sum_q e_q^2 \left(\frac{2}{q}\right)^{1-2i\nu} \frac{\Gamma(1/2 - i\nu)}{\Gamma(1/2 + i\nu)} \int_{-\infty}^{\infty} d\lambda \left(\frac{Q^2}{q^2}\right)^{\frac{-\gamma-i\lambda+1}{2}} \frac{\Gamma(\frac{i\lambda+\gamma-1}{2})}{\Gamma(\frac{-i\lambda-\gamma+3}{2})} \\
&\quad \Gamma\left(\frac{-\gamma-i\lambda}{2} - i\nu + 1\right) \Gamma\left(\frac{-\gamma-i\lambda}{2} + i\nu + 1\right) \int_0^1 d\rho [\rho^2 + (1-\rho)^2] \left(\frac{\rho}{1-\rho}\right)^{\frac{-\gamma+1-i\lambda}{2}} \\
&\quad {}_2F_1\left(1/2 + i\nu, 1/2 - i\nu; \frac{-\gamma-i\lambda+3}{2}; \rho\right) {}_2F_1\left(1/2 + i\nu, 1/2 - i\nu; \frac{\gamma+i\lambda+1}{2}; 1-\rho\right) \quad (3.47)
\end{aligned}$$

and we have used the identity

$$\Gamma(z)\Gamma(1-z) = \frac{\pi}{\sin(z\pi)}. \quad (3.48)$$

The ρ -integration is performed by expanding the first hypergeometric function, performing the integral and then reducing the remaining series using Ψ (digamma) functions. The final result for the non-flip amplitude takes the following form:

$$\begin{aligned}
I_{(+,+)}^\nu(Q^2, q^2) &= \frac{-i}{2} \alpha_s \alpha \pi^5 \sum_q e_q^2 \left(\frac{2}{q}\right)^{1-2i\nu} \frac{1}{\Gamma^2(1/2 + i\nu)} \frac{\tanh(\pi\nu)}{\pi\nu} \frac{1}{(1+\nu^2)} \int_{\gamma-1-i\infty}^{\gamma-1+i\infty} dz \\
&\quad \left(\frac{Q^2}{q^2}\right)^{-z/2} \Gamma(1/2 - i\nu - z/2) \Gamma(1/2 + i\nu - z/2) \Gamma(z/2) \Gamma(z/2 + 1) (z^2 + 11 + 12\nu^2) \quad (3.49)
\end{aligned}$$

and we have changed integration variables to $z = \gamma - 1 + i\lambda$. Of course the $(-, -)$ amplitude is equivalent. For the flip amplitudes we proceed in the same fashion. The final answer is

$$\begin{aligned}
I_{(+,-)}^\nu(Q^2, q^2) &= I_{(-,+)}^\nu(Q^2, q^2) = -2i\alpha_s \alpha \pi^5 \sum_q e_q^2 \left(\frac{2}{q}\right)^{1-2i\nu} \frac{1}{\Gamma^2(1/2 + i\nu)} \frac{\tanh(\pi\nu)}{\pi\nu} \frac{1}{(1+\nu^2)} \\
&\quad \int_{\gamma-1-i\infty}^{\gamma-1+i\infty} dz \left(\frac{Q^2}{q^2}\right)^{-z/2} \Gamma(3/2 - i\nu - z/2) \Gamma(3/2 + i\nu - z/2) \Gamma(z/2) \Gamma(z/2 + 1). \quad (3.50)
\end{aligned}$$

3.1 The limits $Q^2 \gg q^2$ and $Q^2 \ll q^2$

In the limit $Q^2 \gg q^2$ we are able to complete the z integration. We must close the contour in the right half plane. The leading contribution is extracted by considering the left most poles.

For the non-flip amplitude these are located at $z = 1 \pm 2i\nu$:

$$\begin{aligned}
I_{(+,+)}^\nu(Q^2, q^2) \Big|_{Q^2 \gg q^2} &= 2\alpha_s \alpha \pi^6 \sum_q e_q^2 \left(\frac{2}{q}\right)^{1-2i\nu} \frac{1}{\Gamma^2(1/2 + i\nu)} \frac{\tanh(\pi\nu)}{\pi\nu} \frac{1}{(1+\nu^2)} \\
&\quad \left\{ \left(\frac{Q^2}{q^2}\right)^{-1/2-i\nu} \Gamma(-2i\nu) \Gamma(1/2 + i\nu) \Gamma(3/2 + i\nu) [(1+2i\nu)^2 + 11 + 12\nu^2] + c.c. \right\}. \quad (3.51)
\end{aligned}$$

For the flip amplitude, the left most poles are located at $z = 3 \pm 2i\nu$ giving

$$\begin{aligned}
I_{(+,-)}^\nu(Q^2, q^2) \Big|_{Q^2 \gg q^2} &= 8\alpha_s \alpha \pi^6 \sum_q e_q^2 \left(\frac{2}{q}\right)^{1-2i\nu} \frac{1}{\Gamma^2(1/2 + i\nu)} \frac{\tanh(\pi\nu)}{\pi\nu} \frac{1}{(1+\nu^2)} \\
&\quad \left\{ \left(\frac{Q^2}{q^2}\right)^{-3/2-i\nu} \Gamma(-2i\nu) \Gamma(3/2 + i\nu) \Gamma(5/2 + i\nu) + c.c. \right\}. \quad (3.52)
\end{aligned}$$

We see that, in the limit $Q^2 \gg q^2$, the flip amplitude is suppressed by a factor of q^2/Q^2 .

In the limit $Q^2 \ll q^2$ we must close the contour in the left hand plane. The leading piece is found by considering the pole at $z = 0$. This gives the Q^2 independent contribution found in [9]. The first correction to this is found by considering the double pole located at $z = -2$. We find

$$I_{(+,+)}^\nu(Q^2, q^2) \Big|_{Q^2 \ll q^2} = 2\alpha_s \alpha \pi^6 \sum_q e_q^2 \left(\frac{2}{q}\right)^{1-2i\nu} \frac{\Gamma(1/2 - i\nu)}{\Gamma(1/2 + i\nu)} \frac{\tanh(\pi\nu)}{\pi\nu} \frac{1}{(1 + \nu^2)} \left[(11 + 12\nu^2) - (\nu^2 + 1/4) \frac{Q^2}{q^2} (15 + 12\nu^2) \left\{ \ln \frac{|t|}{Q^2} - \frac{8}{15 + 12\nu^2} - \Psi(3/2 + i\nu) - \Psi(3/2 - i\nu) \right\} \right]. \quad (3.53)$$

The analytic structure of the z plane is identical for the flip result and so

$$I_{(+,-)}^\nu(Q^2, q^2) \Big|_{Q^2 \ll q^2} = 8\alpha_s \alpha \pi^6 \sum_q e_q^2 \left(\frac{2}{q}\right)^{1-2i\nu} \frac{\Gamma(1/2 - i\nu)}{\Gamma(1/2 + i\nu)} \frac{\tanh(\pi\nu)}{\pi\nu} \frac{(\nu^2 + 1/4)}{(1 + \nu^2)} \left[1 - (\nu^2 + 9/4) \frac{Q^2}{q^2} \left\{ \ln \frac{|t|}{Q^2} - \Psi(5/2 + i\nu) - \Psi(5/2 - i\nu) \right\} \right]. \quad (3.54)$$

4 $\gamma^* \gamma^* \rightarrow \gamma \gamma$

The cross section for $\gamma^* \gamma^* \rightarrow \gamma \gamma$ scattering can be computed by substituting the results for I^ν given by (3.49) and (3.50) into (2.21). The colour factor for this process is given by

$$G = \frac{N_c^2 - 1}{4} = 2. \quad (4.55)$$

4.1 The small $|t|$ limit

For this process we can study the $|t| \rightarrow 0$ region. The cross section will be greatest in this limit and, interestingly, we can study the behaviour of the amplitude in $|t| \rightarrow 0$ limit. We focus on the limit $Q_1^2 \sim Q_2^2 \gg |t|$ where Q_1^2 and Q_2^2 are the virtualities of the incoming photons. We shall find an analytic approximation for the $\gamma^* \gamma^* \rightarrow \gamma \gamma$ amplitude using the approximation to I^ν given by equation (3.51) and evaluating the ν integration using the saddle point method. We need only consider the non-flip amplitudes. When (3.51) is placed into (2.21) we find two distinct terms. One term is independent of $|t|$ and gives the limiting value of the amplitude when $|t| = 0$. The other term provides the leading $|t|$ dependence. Considering the saddle point integration of the $|t|$ dependent piece we find that the dominant term in the exponential is proportional to $\ln(Q_1^2 Q_2^2 / t^2)$ and so we may make the assumption that the saddle point lies at $\nu \approx \pm i/2$ and approximate $\chi(\nu)$ by an expansion about $\nu = \pm i/2$: $\chi(\nu) \approx 1/(1/2 \pm i\nu)$. The saddle point is in fact at

$$\nu = \pm \frac{i}{2} \left(1 - \sqrt{\frac{4z}{\ln(Q_1^2 Q_2^2 / t^2)}} \right) \approx \pm \frac{i}{2}. \quad (4.56)$$

For the $|t|$ independent piece we have a term proportional to $\ln(Q_1^2 / Q_2^2)$ in the exponential. For $Q_1^2 \sim Q_2^2$ the saddle point is at

$$\nu = \pm \frac{i \ln(Q_1^2 / Q_2^2)}{28\zeta(3)z} \approx 0 \quad (4.57)$$

and we can use $\chi(\nu) \approx 4 \log 2 - 14\zeta(3)\nu^2$. Performing the integration over ν yields

$$A_{(+,+,+,+)}(s, t, Q_1^2, Q_2^2) \Big|_{Q_1^2 \sim Q_2^2 \gg |t|} \approx i \, 9\pi^2 \alpha^2 \alpha_s^2 \left(\sum_q e_q^2 \right)^2 \frac{s}{Q_1 Q_2} \left[\exp \left(4z \ln 2 - \frac{\ln^2(Q_1^2/Q_2^2)}{56\zeta(3)z} \right) \sqrt{\frac{\pi}{14\zeta(3)z}} - \frac{4}{9\pi^{7/2}} \frac{|t|}{Q_1 Q_2} \frac{\ln^{5/4}(Q_1^2 Q_2^2/|t|^2)}{z^{7/4}} \exp \left(2\sqrt{z \ln(Q_1^2 Q_2^2/|t|^2)} \right) \right]. \quad (4.58)$$

There is a cusp in the cross-section at $-t = 0$, i.e. the slope is infinite. In particular, defining an effective b -parameter b_{eff} by

$$b_{\text{eff}} = \frac{2}{A(s, t)} \frac{\partial A(s, t)}{\partial t} \quad (4.59)$$

and using (4.58), we find that, in the vicinity of $-t = 0$,

$$b_{\text{eff}} = \frac{1}{A_0} \frac{4}{9\pi^{7/2}} \frac{1}{Q_1 Q_2} \exp \left(2\sqrt{z \ln(Q_1^2 Q_2^2/|t|^2)} \right) \frac{\ln^{5/4} \left(\frac{Q_1^2 Q_2^2}{-t} \right)}{z^{7/4}} \quad (4.60)$$

where

$$A_0 \approx e^{4z \ln 2} \sqrt{\frac{\pi}{14\zeta(3)z}}. \quad (4.61)$$

4.2 The large $|t|$ limit

We now consider the limit $Q_1^2, Q_2^2 \ll |t|$. The saddle point is at $\nu = 0$ and, after integration over ν , we find that

$$\begin{aligned} A_{(+,+,+,+)}(s, t, Q_1^2, Q_2^2) \Big|_{|t| \gg Q_1^2, Q_2^2} &= \frac{i}{4} \pi \frac{s}{|t|} \alpha^2 \alpha_s^2 \left(\sum_q e_q^2 \right)^2 e^{4z \ln 2} \left(\frac{\pi}{14\zeta(3)z} \right)^{3/2} C_1(Q_1) C_1(Q_2) \\ A_{(+,-,+,+)}(s, t, Q_1^2, Q_2^2) \Big|_{|t| \gg Q_1^2, Q_2^2} &= \frac{i}{4} \pi \frac{s}{|t|} \alpha^2 \alpha_s^2 \left(\sum_q e_q^2 \right)^2 e^{4z \ln 2} \left(\frac{\pi}{14\zeta(3)z} \right)^{3/2} C_2(Q_1) C_2(Q_2) \end{aligned} \quad (4.62)$$

where

$$\begin{aligned} C_1(Q_1) &= 11 + \frac{1}{4} \frac{Q_1^2}{|t|} \left(68 - 30\gamma_E - 60 \ln 2 - 15 \ln \left(\frac{|t|}{Q_1^2} \right) \right) \\ C_2(Q_1) &= 1 - \frac{9}{4} \frac{Q_1^2}{|t|} \left(-\frac{16}{3} + 2\gamma_E + 4 \ln 2 + \ln \left(\frac{|t|}{Q_1^2} \right) \right). \end{aligned} \quad (4.63)$$

The amplitudes $A_{(+,+,+,-)}$ and $A_{(+,-,+,+)}$ have a similar form, the final factors being replaced by $C_1(Q_1)C_2(Q_2)$ and $C_2(Q_1)C_1(Q_2)$ respectively.

4.3 Numerical results

In Fig.3 we show the results for the $\gamma^* \gamma^* \rightarrow \gamma \gamma$ differential cross-section obtained using equations (3.49) and (3.50) and compare with the results obtained using the approximations to $I_{(+,+)}^\nu$ and $I_{(+,-)}^\nu$ given in (3.51), (3.52), (3.53) and (3.54). All ν integrals are computed numerically.

At LEP2, z values around 1 are typical and values of around 2 are more typical of those attainable at a future linear collider.

5 $\gamma^* P \rightarrow \gamma X$

We may use the results (3.49) and (3.50) to compute $\gamma^* \rightarrow \gamma$ scattering off a hadronic state. We consider $\gamma^* P \rightarrow \gamma X$ scattering at the energies typical of those at the HERA collider.

The impact factor for the coupling to the quarks and gluons in the proton is well known [2, 16] and yields

$$I_q^\nu = -2(2\pi)^5 \alpha_s \frac{\Gamma(1/2 - i\nu)}{\Gamma(1/2 + i\nu)} \left(\frac{2}{q}\right)^{1-2i\nu} \quad (5.64)$$

for the coupling to quarks. The colour factor for coupling to quarks is

$$G = \frac{N_c^2 - 1}{4N_c} = 2/3,$$

relative to which the coupling to gluons is enhanced by a factor $C_A/C_F = 9/4$. Putting the colour factor, along with (3.49), (3.50), (5.64), into (2.21) yields

$$\begin{aligned} A_{(+,+)}(s, t, Q^2) &= i \alpha \alpha_s^2 \sum_q e_q^2 \frac{\pi}{6} \frac{s}{|t|} \int d\nu \frac{\nu^2}{(1/4 + \nu^2)^2} \frac{1}{1 + \nu^2} \frac{\tanh(\pi\nu)}{\pi\nu} e^{z\chi(\nu)} \\ &\int_{\gamma-1-i\infty}^{\gamma-1+i\infty} \frac{dz}{2\pi i} \left(\frac{Q^2}{|t|}\right)^{-z/2} \frac{\Gamma(1/2 - i\nu - z/2) \Gamma(1/2 + i\nu - z/2)}{\Gamma(1/2 + i\nu) \Gamma(1/2 - i\nu)} \Gamma(z/2) \Gamma(z/2 + 1) [z^2 + 11 + 12\nu^2] \end{aligned} \quad (5.65)$$

and

$$\begin{aligned} A_{(+,-)}(s, t, Q^2) &= i \alpha \alpha_s^2 \sum_q e_q^2 \frac{2\pi}{3} \frac{s}{|t|} \int d\nu \frac{\nu^2}{(1/4 + \nu^2)^2} \frac{1}{1 + \nu^2} \frac{\tanh(\pi\nu)}{\pi\nu} e^{z\chi(\nu)} \\ &\int_{\gamma-1-i\infty}^{\gamma-1+i\infty} \frac{dz}{2\pi i} \left(\frac{Q^2}{|t|}\right)^{-z/2} \frac{\Gamma(3/2 - i\nu - z/2) \Gamma(3/2 + i\nu - z/2)}{\Gamma(1/2 + i\nu) \Gamma(1/2 - i\nu)} \Gamma(z/2) \Gamma(z/2 + 1). \end{aligned} \quad (5.66)$$

5.1 The low Q^2 limit

In the limit $-t \gg Q^2$ the saddle point integration about $\nu = 0$ yields

$$A_{(+,+)}(s, t, Q^2) \Big|_{Q^2 \ll |t|} = \frac{8i}{3} \alpha \alpha_s^2 \sum_q e_q^2 \frac{s}{|t|} e^{4z \ln 2} \left(\frac{\pi}{14z\zeta(3)}\right)^{3/2} C_1(Q) \quad (5.67)$$

and

$$A_{(+,-)}(s, t, Q^2) \Big|_{Q^2 \ll |t|} = \frac{8i}{3} \alpha \alpha_s^2 \sum_q e_q^2 \frac{s}{|t|} e^{4z \ln 2} \left(\frac{\pi}{14z\zeta(3)}\right)^{3/2} C_2(Q). \quad (5.68)$$

5.2 The high Q^2 limit

The relevant saddle point is now at $\nu \approx \pm i/2$ and so

$$A_{(+,+)}(s, t, Q^2) \Big|_{Q^2 \gg |t|} = \frac{8i}{3\sqrt{\pi}} \alpha \alpha_s^2 \sum_q e_q^2 \frac{s}{Q^2} \frac{\ln^{3/4}(Q^2/|t|)}{z^{5/4}} \exp \left(2\sqrt{z \ln(Q^2/|t|)} \right) \quad (5.69)$$

and

$$A_{(+,-)}(s, t, Q^2) \Big|_{Q^2 \gg |t|} = \frac{16i}{9\sqrt{\pi}} \alpha \alpha_s^2 \sum_q e_q^2 \frac{s|t|}{Q^4} \frac{\ln^{3/4}(Q^2/|t|)}{z^{5/4}} \exp \left(2\sqrt{z \ln(Q^2/|t|)} \right) \quad (5.70)$$

The dominance of the non-flip amplitude over the flip amplitude is clear:

$$\frac{A_{(+,+)}}{A_{(+,-)}} = \frac{3Q^2}{2|t|}. \quad (5.71)$$

5.3 Numerical Results

In Fig.4 we show the results for proton-photon scattering in by performing the ν and z integrals exactly. We compare with the results obtained using the analytic approximations to the amplitude derived from (3.52),(3.51),(3.54), (3.53) again with the ν integral performed exactly.

The proton-photon cross section is determined by convoluting the photon-quark cross section with the parton density functions [17, 18]:

$$\frac{d\sigma(\gamma P \rightarrow \gamma X)}{dt} = \int_{x_{\min}}^1 dx \left(\frac{81}{16} g(x, t) + \sum_f (q(x, t) + \bar{q}(x, t)) \right) \frac{d\sigma(\gamma q \rightarrow \gamma q)}{dt}. \quad (5.72)$$

The lower limit of the x integral is determined by the on-shell condition for the struck quark in the proton, i.e.

$$x_{\min} = \frac{1}{(\frac{M_X^2}{|t|} + 1)}, \quad (5.73)$$

where M_X is the maximum invariant mass of the proton dissociation products. We choose $M_X = 10$ GeV, which is typical of the cuts imposed by the HERA experiments. We note that in the limit of $|t| \gg Q^2$ the cross section becomes insensitive to values of Q^2 , as anticipated in the analytic expressions (5.67) and (5.68). The approximate expressions are shown to be good over a large range in $Q^2/|t|$. We note that these cross-sections are large enough to make observation at HERA feasible.

6 Acknowledgements

We wish to thank Mark Wüsthoff for many long and detailed discussions. NGE was funded for this work from a PPARC studentship. This work was supported in part by the EU Fourth Programme ‘Training and Mobility of Researchers’, Network ‘Quantum Chromodynamics and the Deep Structure of Elementary Particles’, contract FMRX-CT98-0194 (DG 12-MIHT).

References

- [1] J.R. Forshaw and P.J. Sutton, Euro. Phys. J **C14** (1998) 285.
- [2] A.H. Mueller and W-K. Tang, Phys. Lett. **B284** (1992) 123.
- [3] B.E. Cox and J.R. Forshaw, Phys. Lett. **B434** (1998) 133.
- [4] ZEUS Collaboration: M.Derrick et al, Phys. Lett **B369** (1996) 55;
H1 Collaboration: “Rapidity Gaps Between Jets in Photoproduction at HERA” contribution to The International Europhysics Conference on High Energy Physics, Jerusalem, Israel, August 1997;
H1 Collaboration: “Double Diffraction Dissociation at large $|t|$ in Photoproduction at HERA” contribution to ICHEP98, Vancouver, Canada, July 1998;
CDF Collaboration: F.Abe. et al, Phys. Rev. Lett. **74** (1995) 855;
D0 Collaboration: S. Abachi et al, Phys. Rev. Lett. **76** (1996) 734.
- [5] I.F. Ginzburg, S.L. Panfil, V.G. Serbo, Nucl. Phys **B284** (1987) 685.
- [6] I.F. Ginzburg and D.Yu. Ivanov, Phys. Rev. **D54** (1996) 5523.
- [7] J.R. Forshaw and M.G. Ryskin, Zeit. Phys. **C68** (1995) 137;
J. Bartels, J.R. Forshaw, H. Lotter, M. Wüsthoff, Phys. Lett. **B375** (1996) 301;
D.Yu. Ivanov, Phys. Rev. **D53** (1996) 3564;
D.Yu. Ivanov and R. Kirschner, Phys. Rev. **D58** (1998) 4026.
- [8] H1 Collaboration: “Production of J/Ψ Mesons with large $|t|$ at HERA” contribution to The International Europhysics Conference, Jerusalem, Israel, August 1997;
ZEUS Collaboration: “Study of Vector Meson Production at Large $|t|$ at HERA” contribution to The International Europhysics Conference, Jerusalem, Israel, August 1997;
ZEUS Collaboration: “Study of Vector Meson Production at Large $|t|$ at HERA and Determination of the Pomeron Trajectory” contribution to ICHEP98, Vancouver, Canada, July 1998.
- [9] D.Yu. Ivanov and M. Wüsthoff, preprint hep-ph/9808455.
- [10] J. Bartels, A. De Roeck, H. Lotter, Phys. Lett. **B389** (1996) 742;
S.J. Brodsky, F. Hautmann, D.E. Soper, Phys. Rev. **D56** (1997) 6957;
S.J. Brodsky, F. Hautmann, D.E. Soper, Phys. Rev. Lett. **78** (1997) 803; Erratum-ibid. **79** (1997) 3544.
- [11] Ya.Ya. Balitsky and L.N. Lipatov, Sov. J. Nucl. Phys. **28** (1978) 822;
E.A. Kuraev, L.N. Lipatov, V.S. Fadin, Phys. Lett. **B60** (1975) 5; Sov. Phys. JETP **71** (1976) 840; Sov. Phys. JETP **72** (1977) 377.
- [12] L.N. Lipatov, Sov. Phys. JETP **63** (1986) 904.
- [13] L.N. Lipatov and G.V. Frolov, Sov. J. Nucl. Phys. **13.3** (1971) 333;
H. Cheng and T.T. Wu, Phys. Rev. **D1.123** (1970) 3414.

- [14] J.R. Forshaw and D.A. Ross, ‘QCD and the Pomeron’, Cambridge University Press (1997).
- [15] J.A.M. Vermaseren, ‘Symbolic Manipulation with FORM, Tutorial and Reference Manual’, CAN[†] (1991).
- [16] J. Bartels, J.R. Forshaw, H. Lotter, L.N. Lipatov, M.G. Ryskin, M. Wüsthoff, Phys. Lett. **B348** (1995) 589.
- [17] H. Plathow-Besch, Comp. Phys. Comm. **75** (1993) 396;
H. Plathow-Besch, Int. J. Mod. Phys. **A10** (1995) 2901.
- [18] A.D. Martin, R.G. Roberts, W.J. Stirling, Phys. Rev. **D51** (1995) 4756.

[†]e-mail:form@can.nl

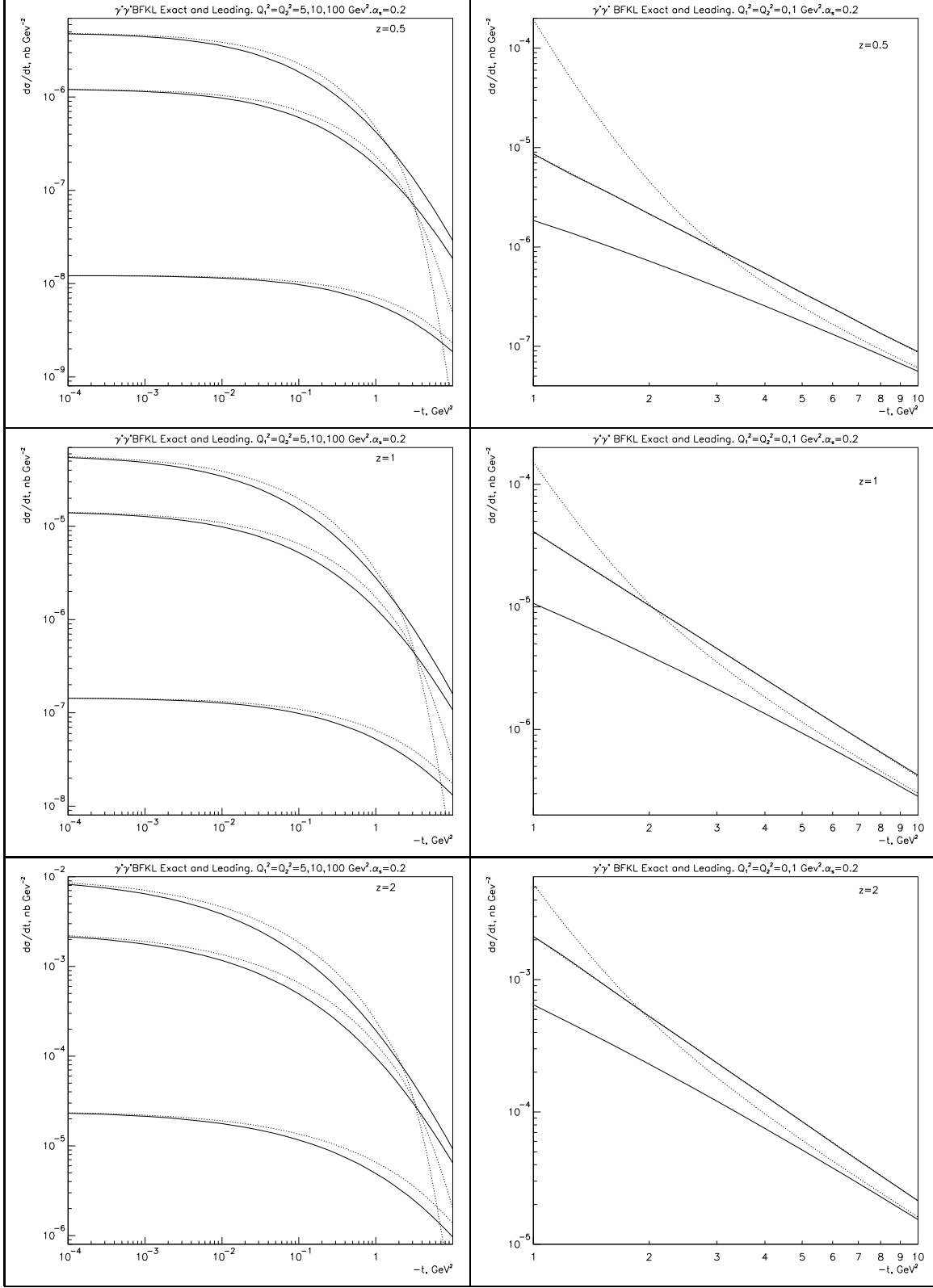


Figure 3. $\gamma^*\gamma^* \rightarrow \gamma\gamma$ cross section comparing the exact BFKL result with the leading approximation. The solid line gives the exact result and the dotted line the result obtained by only keeping the leading terms as described in the text.

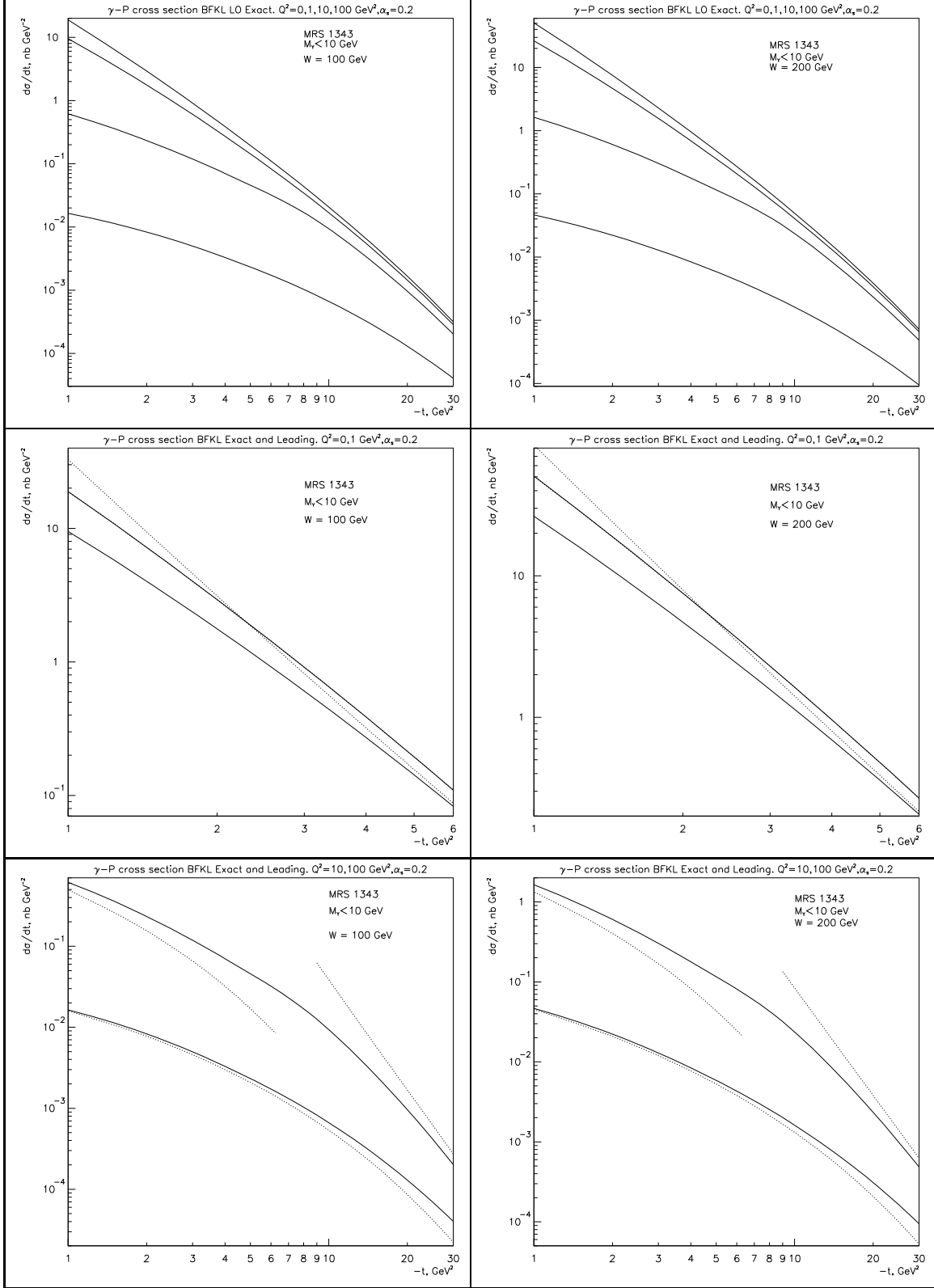


Figure 4. $\gamma^*P \rightarrow \gamma X$ cross section comparing the exact BFKL result with the leading approximation. The solid line gives the exact result and the dotted line the result obtained by only keeping the leading terms as described in the text.